PAPER

Check for updates

Application of amino-hypophosphite polyampholyte for purification of wastewater containing Ni(II) ions†

Justyna Ulatowska, [ID] * Łukasz Stala, [ID] Natasza Trzęsowska and Izabela Polowczyk [ID]

This study investigated the sorption of Ni(II) ions from an aqueous solution using novel, synthetic amino-hypophosphite polyampholyte resin (AHP) in a batch adsorption system. The removal of Ni(II) ions was determined as a function of pH (2.0–8.0), initial concentration of Ni(II) ions (2.0–20.0 mM), resin dosage (1.0–10.0 g dm^{-3}), contact time (0.04–24 h), and temperature (298–318 K). Moreover, continuous fixed-bed column sorption was also studied using model solutions and actual wastewater from the galvanising plant. The batch sorption experimental data showed that the maximum pH for efficient Ni(II) ion removal was about 5.0. An equilibrium was reached after about 24 hours. The kinetics results were fitted using pseudo-first-order (PFO), pseudo-second-order (PSO), liquid film (LFD), and intraparticle diffusion (IPD) models. Freundlich and Langmuir isotherm models were applied for sorption equilibrium data. The maximum sorption capacity was obtained from the Langmuir equation to be 2.39, 2.52, and 2.62 mmol g^{-1} at 298, 308, and 318 K, respectively. The thermodynamic parameters for the sorption of Ni(II) ions on AHP imply the endothermic and spontaneous character of the process. The experimental results demonstrated that amino-hypophosphite polyampholyte resin could be used to effectively remove Ni(II) ions from model solutions and real wastewater.

1. Introduction

The classification of metal ions pollution by source distinguishes two groups of sources: natural and anthropogenic.[1] The natural source of heavy metals, deposits, is less environmentally harmful as it does not threaten higher organisms.[2] The anthropogenic source is, however, much more significant. Human activities such as fossil fuel combustion, agriculture, mineral processing, and industrial wastewater generation release toxic metals directly into the environment,[3] causing bioaccumulation of those elements.[2] This, in the case of heavy metals, intensifies their harmfulness. The anthropogenic introduction of heavy metals into the environment, starting with extraction, processing, and disposal, is now widespread and increasing.

Currently, IUPAC does not provide a strict definition of heavy metals. It is widely accepted that elements included in this group are characterized by high density (lower limit of about 3–6 g cm^{-3}), an atomic number above 20, and high atomic mass.[4] The most commonly occurring metals considered members of this group are manganese, chromium, cadmium, copper, and nickel.[5] Nickel is

the fifth most common element in the Earth's crust by mass. The most significant deposits are located in Canada, Siberia and New Caledonia.[6] Furthermore, it is estimated that around 8 billion tons of nickel are dispersed in the seas and oceans.[7] In the bound form, nickel predominantly occurs in the second oxidation state.[8]

Heavy metals are known to have a detrimental impact on living organisms. In lower doses, they are essential for plant growth and development.[9] However, as the concentration increases, so does the toxicity. In the long run, exposure to toxic metals can cause serious damage, such as various types of cancer,[10,11] multiple sclerosis,[9] and Alzheimer's disease.[12,13] In the case of nickel, higher doses contribute to diseases of the respiratory tract, kidneys, and cardiovascular system.[7] Another important issue is metal-triggered allergic reactions, where nickel is estimated to cause 15% of all cases.[14]

All of these harmful effects point to the need for heavy metal removal. For water purification, various methods are available, ranging from adsorption, biosorption, ion exchange, and chemical precipitation to membrane techniques (reverse osmosis, electrodialysis, ultra-, and nanofiltration).[15,16] This study focuses on ion exchange as a promising technique for Ni(II) ion removal. The most important characteristics of this method are the lack of sludge production,[17] fast kinetics,[18] metal selectivity,[19] and convenient recovery of ion exchangers.[20] The materials used in this method should have an open network that allows for ion migration. Zeolites, animal and plant cells,[21] acidic salts of multivalent metals,[22] and synthetic

Department of Process Engineering and Technology of Polymer and Carbon Materials, Faculty of Chemistry, Wroclaw University of Science and Technology, Norwida 4/6, Wroclaw 50–373, Poland. E-mail: justyna.ulatowska@pwr.edu.pl; Tel: +48-713-203-206

resins[23] are only a few examples from the broad group of ion exchangers.

Ion exchanger and metal scavenger markets are currently dominated by products based on styrene/divinylbenzene copolymers.[24,25] These products are functionalised resins bearing aminomethylphosphonic and iminediacetic groups that are known for their metal chelating properties.[26] There are commercial products based on siloxane structures that can be used alternatively to crude-oil-based products. Over the years, countless experimental scavenging materials were studied, varying in matrix composition and functional group type. In the last two decades, countless works have been published on novel materials for adsorption and ion exchange (Table S1 in ESI† with references). There is a recent trend of fulfilling green chemistry and sustainability principles in materials production, addressing the importance of circular economy in current technology. There is a very limited amount of papers on metal scavengers with dimethylhypophosphite fragments in their structure. In our previous work,[27] we reported that a group of amino-hypophosphite polyampholytes (AHPs) can be used as metal scavengers with high efficiency from Cu(II) containing model wastewater. In that study, batch mode experiments were conducted to reveal the chemistry behind the Cu(II) removal on AHP. This work presents the performance of bis(hexamethylene) triamine-based AHP in Ni(II) removal from wastewater sourced at a local galvanising plant (Wrocław, Poland), both in batch and column modes.

In this study, the removal of Ni(II) ions from aqueous solutions using an amino-hypophosphite polyampholyte (AHP) was investigated. The resin produced was characterised in detail. The main objectives of the research were the following four consecutive steps:

1. kinetic study and understanding of the kinetic mechanism;
2. static study of removal of Ni(II) ions on resin;
3. dynamic study of the column flow removal;
4. treatment of real wastewater.

For these aims, different parameters affecting the sorption process, such as the initial pH of a solution, contact time, resin dosage, temperature and initial Ni(II) ion concentration, were analysed. Finally, the treatment of the model and real wastewater in a fixed bed column was conducted.

2. Materials and methods

2.1. Materials

The chemicals used in this study were listed in ESI† along with data on purity and supplier details.

The galvanic wastewater was sourced from the local galvanising plant based in Wroclaw (Poland), which specialises in nickel plating and chrome plating. The galvanic bath used in this plant is a Watts type bath, mainly containing nickel(II) sulfate, nickel(II) chloride, and boric acid. The bath solutions were analysed to estimate concentrations of selected components such as nickel(II), iron(II), chromium, and others. The chemical composition of wastewater analysed with the ICP-MS technique is presented in Table 1.

2.2. Physicochemical characteristics of the resin

The characterisation of obtained resin was performed through BET and XPS analyses and measurements of SEM micrographs. Metal ion concentrations were measured using ICP MS method. The specific information on the equipment used for characterisation was provided in ESI.†

2.3. Methodology

2.3.1. Preparation of amino-hypophosphite polyampholyte. Bis(6-aminohexyl)amine (0.100 moles, 21.60 g) was dissolved in water (36.0 cm³) at room temperature, and 12 M hydrochloric acid was used to adjust the pH below 2. The mixture was then stirred until hydrochloric acid vapours faded. Then sodium hypophosphite (0.25 moles, 26.5 g) was added, followed by water (26.0 cm³) and 12 M hydrochloric acid (0.25 moles, 20.9 cm³). Shortly after paraformaldehyde mixture (0.90 moles, 27.00 g) in water (46.0 cm³) was added. The solution was stirred for 1.5 h at 373 K. AHP synthesis was carried out according to the following reaction, eqn (1):
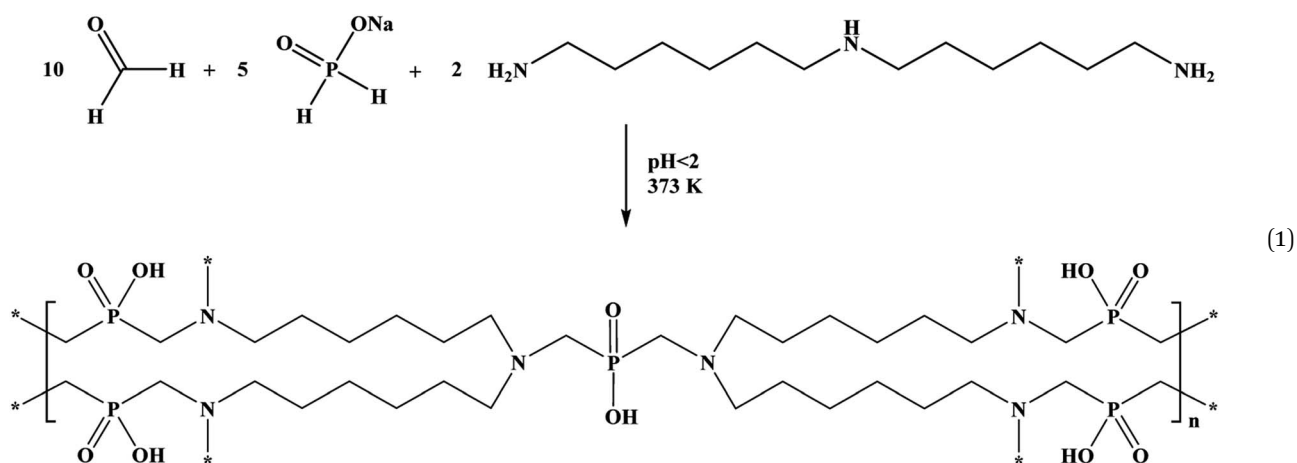

$$\tag{1}$$

Table 1 Composition of galvanic wastewater sourced at Wroclaw-based galvanising plant

Analysed ion	Concentration (mg dm^{-3})
Ni	1024
Cr	1.95
Co	3.10×10^{-3}
Fe	0.10×10^{-3}

The reaction was controlled using the ^{31}P NMR spectra until the hypophosphite fragments in the leftover solution were built into the resin's structure. The obtained product was washed with deionised water to rinse out the excess residual substrates or impurities generated in the reaction. The rinsing was continued until the pH of the effluent was no longer strongly acidic. The product was dried in laboratory air drier at 373 K. The polymeric product's formula and molecular weight are $(C_{35}H_{76}N_6O_{10}P_5)_n$ and 894.9 g mol^{-1}, respectively. The reaction yield was over 99%, according to gravimetric analysis.

2.3.2. Model Ni(II) solution. Nickel (II) chloride (NiCl$_2$·6H$_2$O) was used as the source of Ni(II) ions. A stock solution (20 mM) was prepared in demineralised water in the presence of sulfuric acid. The concentration of Ni(II) was analysed spectrophotometrically using the dimethylglyoxime method, according to the standard procedure.

2.3.3. Removal of Ni(II) ions

2.3.3.1 Kinetic sorption. A specific mass of adsorbent (AHP) was flooded into 100 cm^3 of 20 mM Ni(II) ion solution to obtain the appropriate resin concentration (4 mg dm^{-3}). The suspensions were mixed and placed in a thermostated rotary shaker (200 rpm). Samples were drawn for analysis of Ni(II) ions at the following periods: 2.5; 5; 10; 20; 40; 80; 160; 320; 600, and 1440 min. The experiments were carried out at a set temperature of 298 K.

2.3.3.2 Static sorption

2.3.3.2.1 Effect of pH. The determined resin mass (40 mg) was contacted with 10 cm^3 of 10 mM Ni(II) ion solution to obtain an adsorbent concentration of 4 g dm^{-3}. The pH of the Ni(II) ion solution was then determined to range from 2 to 8 using 0.1 M HCl solution and 0.1 M NaOH solution. The resulting suspensions were mixed and placed in a laboratory rotator for 24 h (200 rpm, 298 K).

2.3.3.2.2 Effect of resin dosage. Specific resin masses were contacted with 10 cm^3 of 20 mM Ni(II) ion solution to obtain adsorbent concentrations ranging from 1 to 10 g dm^{-3} and to set the pH of the solution at about 5.0. The resulting suspensions were mixed and placed in a laboratory rotator for 24 h (200 rpm, 298 K).

2.3.3.2.3 Effect of initial Ni(II) ion concentration. A specific resin mass (40 mg) was contacted with a 10 cm^3 solution of Ni(II) ions at concentrations ranging from 2 to 20 mM, obtaining an adsorbent concentration of 4 g dm^{-3} and fixing the pH of the solution at about 5.0. The suspensions were mixed and placed in a temperature-controlled rotary shaker (200 rpm) for 24 h at the specified temperature: 298 K, 308 K or 318 K.

2.3.3.3 Dynamic sorption. The dynamics of Ni(II) ion sorption were studied in a vertical glass column. A schematic diagram of the adsorption column is shown in Fig. 1. The column, 0.10 m long and with 0.010 m inner diameter, was provided with a sinter at the bottom. The sinter allowed the resin to be retained, but its presence did not affect the course and efficiency of the process. The peristaltic pump, which introduced the Ni(II) ion solution above, ensured the same hydrostatic conditions in the column (constant solution level above the fixed bed). For the column tests, 1.5 g of resin was used. The initial concentration of Ni(II) ions in the solution was 11 mM, and the solution was dispensed into the column at a flow rate of 0.020 cm^3 s^{-1}. The total process running time in the fixed bed column was about 2 h. To determine the adsorption front, the Ni(II) ion solution was sampled over time during the process – initially, every 1 min and then every 5 min, until the Ni(II) ion concentration in the solution was approximately 95% of the initial Ni(II) ion solution concentration.

All column measurements were made under the following assumptions: only one component of the flux is retained (in this case, Ni(II) ions); the loss of the adsorbate in time does not change the viscosity and density values of the stream; the process is isothermal (T = 298 K); the stream moves in one direction at a constant speed; measurements are carried out until the Ni(II) ion concentration at the column outlet (c_t) is 95% of the concentration entering the column (c_0).

The process of removing Ni(II) ions from an aqueous solution was carried out in a five-fold cycle involving 3 purification cycles and 2 fixed bed regeneration cycles. This enabled the effectiveness of the resin regeneration to be tested and reapplied to remove Ni(II) ions from the solution without removing the bed from the column. The bed regeneration process was carried out
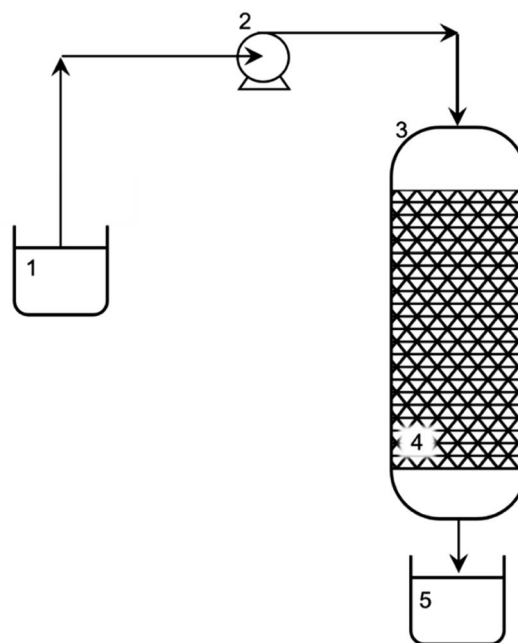

Fig. 1 Experimental setup for sorption of Ni(II) from aqueous solution: 1 – influent (stock solution of Ni(II): 11 mM); 2 – peristaltic pump; 3 – glass column; 4 – fixed bed (AHP); and 5 – effluent.

using a 25 mM HCl solution introduced into the column at a flow rate of 0.019 cm^3 s^{-1}. The column was then washed with deionized water at a flow rate of 0.019 cm^3 s^{-1}. The washing was continued until pH reached 6. A schematic diagram of the experimental setup for removing Ni(II) ions from an aqueous solution is shown in Fig. 1.

2.3.4. Real wastewater treatment. In this experiment, effluent collected from a local electroplating plant was used as an exhausted Watts bath with an initial Ni(II) concentration of 1024 mg dm^{-3}. The glass column was loaded with 5 g of AHP. The experiment continued until the column effluent concentration performed 95% of the nickel concentration in the feed. The column was then flushed with distilled water, and 50 cm^3 of the 6 M hydrochloric acid was directed to the column. The fractions were then collected in test tubes, and Ni(II) concentrations were measured. The samples with Ni(II) were mixed, and 37 cm^3 of concentrate was obtained containing 270 mg Ni(II). The column was further flushed with 50 cm^3 1 M hydrochloric acid. Then 100 cm^3 of 1 M sodium hydroxide was directed to the column, followed by distilled water to flush sodium chloride and residual sodium hydroxide. The column was then ready for the next cycle.

2.4. Mathematical formulas used

The sorption Ni(II) capacity of AHP was calculated using eqn (2):

$$q = \frac{(c_0 - c) \cdot V}{m} \tag{2}$$

The Ni(II) percentage removal was calculated using eqn (3):

$$PR = \left(\frac{c_0 - c}{c_0}\right) \cdot 100\% \tag{3}$$

All formulas for the mathematical kinetic and equilibrium models used are summarised in Table S2 in ESI.†

3. Results

3.1. Characterization of amino-hypophosphite polyampholyte

The morphology of AHP materials was registered using a digital camera and SEM apparatus. The images obtained are shown in

Table 2 Characteristic data of amino-hypophosphite polyampholyte (AHP)

Characteristic	Value
Appearance	Yellow
Ionic forms (H$^+$ or Na$^+$)	H$^+$
Temperature limitations (K)	298–328[a]
Structure	gel
Matrix	Ampholytic, polycondensate crosslinked by methyl groups
Functional group	Phosphate groups
Surface area (m^2 g^{-1})	0.204
Density (g dm^{-3})	2570
Bulk density (g dm^{-3})	770
Total exchange capacity for Ni(II) (mmol g^{-1})	2.85

[a] The AHP was tested in this temperature range. There are no data on how the material behaves in temperatures below or above this range.

Fig. 2. Table 2 provides the summary of the physical and chemical properties of the produced material.

After the successful synthesis of amino-hypophosphite polyampholyte resin, the XPS analysis confirmed that the obtained
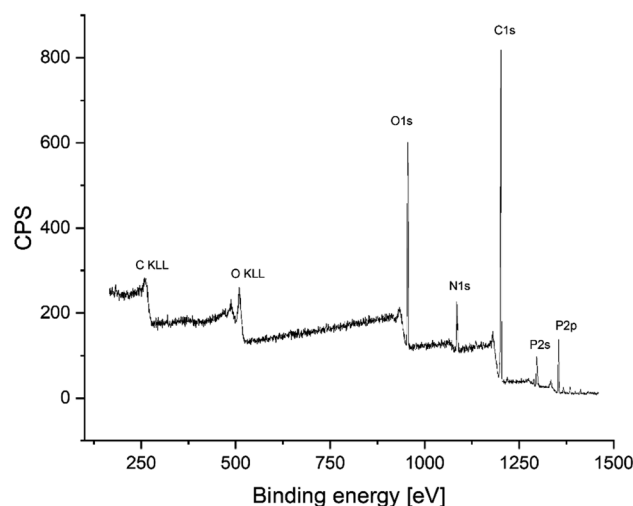

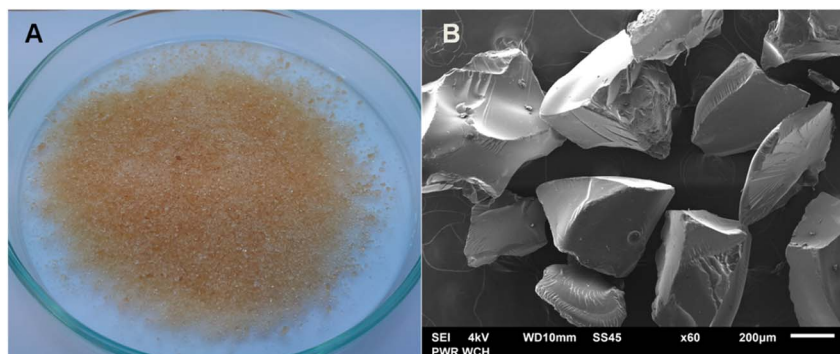**Fig. 3** XPS survey scan of amino-hypophosphite polyampholyte (AHP).

Fig. 2 Images of synthetic AHP taken with a digital camera (A) and a scanning electron microscope (B).

Table 3 Calculated atomic composition from XPS survey with a comparison with an atomic concentration based on a theoretical structure derived from reaction eqn (1)

Name (−)	Position (−)	Raw area (a.u.)	Atomic concentration XPS(%)	Atomic concentration calculated (%)
C 1s	284.6	1838.1	64.6	62.5
O 1s	531.3	1475.1	17.7	17.9
N 1s	399.2	395.5	9.1	10.7
P 2p	132.1	292.1	8.6	8.9

materials possess functional groups that should be present in the AHP structure. The obtained XPS spectrum is shown in Fig. 3.

A comparison of the calculated atomic composition from the XPS study with the atomic concentration based on the theoretical structure derived from reaction eqn (1) is summarized in Table 3.

The XPS-derived atomic compositions of elements in the amino-hypophosphite polyampholyte match the calculated compositions from the theoretical structure based on the Moedritzer–Irani reaction. The small difference in carbon content in XPS analysis can be explained by the presence of terminal methyl groups that can be produced in excess of formaldehyde, which must be used in the reaction for optimal crosslinking of the AHP structure. The FTIR spectra of the obtained amino-hypophosphite polyampholyte was added in ESI as Fig. S1† with signal assignment with references from literature. Fourier-transform Infrared (FTIR) spectrum showed distinctive bands at 3600–3200, 3000–2750, 2400–2150, 1668, 1643, 1467, 1180, 1054, 1026 and 840 cm^{-1}.

3.2. Removal of nickel ions

3.2.1. Sorption kinetics. In Fig. 4 the removal of Ni(II) ions was shown as a function of contact time. It can be noticed that the removal efficiency was rapid in the initial stages of the

process and that equilibrium was stabilised after 24 hours. Although the difference between the removal efficiency of Ni(II) ions on AHP after 20 hours (52.1%) and 24 hours (53.0%) was insignificantly small, it was decided that all batch experiments would be performed within 24 hours to ensure that an equilibrium state was reached.

Two kinetic models were analysed (pseudo-first order (PFO) and pseudo-second order (PSO)) in order to provide information on the mechanism of Ni(II) removal in the process. The mathematical notation of these equations is given in Table S1.† The slopes and intersection points with the Y-axis of these curves were used to determine the model parameters k_1 and k_2 and the equilibrium capacity q_1 and q_2, respectively, for the PFO and PSO models. The calculated value of the equilibrium capacity from the PFO model (q_1) was lower than the experimental value (q_{exp}). A better agreement was obtained between the model and experimental values in the PSO kinetic model (q_2). As a result, the high value of the Pearson correlation coefficient ($R^2 > 0.995$) and good coherence between the experimental and calculated values of q_t show that the PSO model describes accurately the removal of Ni(II) ions in the present study. The calculated parameters of both kinetic models and the R^2 are summarized in Table 4.

The mechanism of Ni(II) ion removal on AHP, according to the literature, can proceed in four basic steps:[28,29] (1) transport of Ni(II) ions from the bulk solution into the liquid film near the resin surface, (2) diffusion of Ni(II) ions through the liquid film to the resin surface, (3) sorption of Ni(II) onto active sites on the surface, and 4. diffusion of Ni(II) ions through the particle. A fifth step involving chemical reaction is also distinguished in some cases.[28] The step that controls the overall process is the slowest stage. Supposing that the concentration of ions removed in the solution is not extremely low, the process rate can be controlled by either diffusion in the liquid layer or
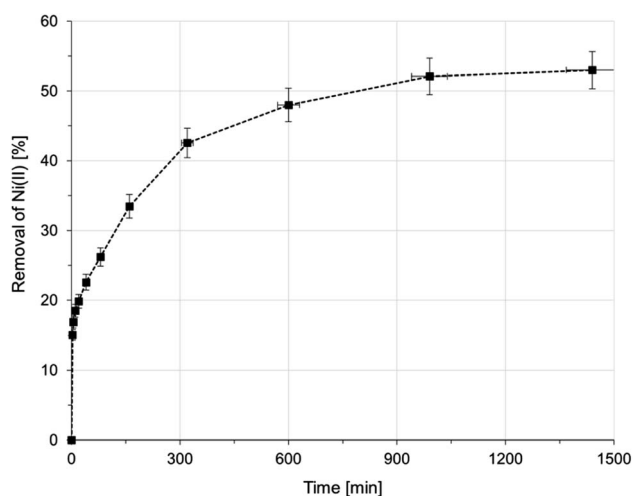

Fig. 4 Sorption of Ni(II) onto AHP as a function of time (initial Ni(II) concentration: 20 mM; concentration of resin: 4 mg dm^{-3}; 298 K; pH 5.0).

Table 4 Kinetic parameters of Ni(II) removal on AHP

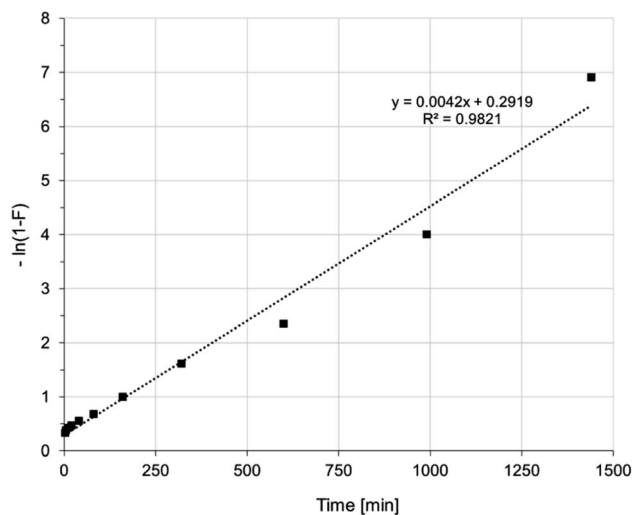| Models	Parameters	Values
PFO	q_{exp} (mmol g^{-1})	2.65
	k_1 (min^{-1})	4.23×10^{-3}
	q_1 (mmol g^{-1})	1.98
	R^2 (−)	0.982
PSO	k_2 (g mmol^{-1} min^{-1})	8.63×10^{-3}
	q_2 (mmol g^{-1})	2.69
	h (mmol g^{-1} min^{-1})	6.24×10^{-2}
	R^2 (−)	0.995

RSC Advances

Paper

Fig. 5 Liquid film diffusion model of Ni(II) sorption on AHP (initial Ni(II) concentration: 20 mM; concentration of resin: 4 mg dm^{-3}; 298 K; pH 5.0).

intraparticle diffusion. A linear plot of $-\ln(1 - F)$ vs. t (where F is the fractional attainment of equilibrium) with a zero intercept suggests that the kinetics of the process is controlled by diffusion in the liquid film.[30] Fig. 5 shows that applying the diffusion model in the liquid film to the obtained experimental data does not yield a straight line passing through the origin of the coordinate system. Hence, diffusion in the liquid film is not a rate-determining step in the overall process. Fig. 6 shows the intraparticle diffusion model fit for Ni(II) sorption experiment. The curves display three separate curves with three slopes and intercept values for the AHP indicating three stages of the diffusion disturbance of the process. The first stage is related to the film diffusion, the second stage is a result of intraparticle diffusion influence on the process, and the third stage indicates the saturation stage.[31]
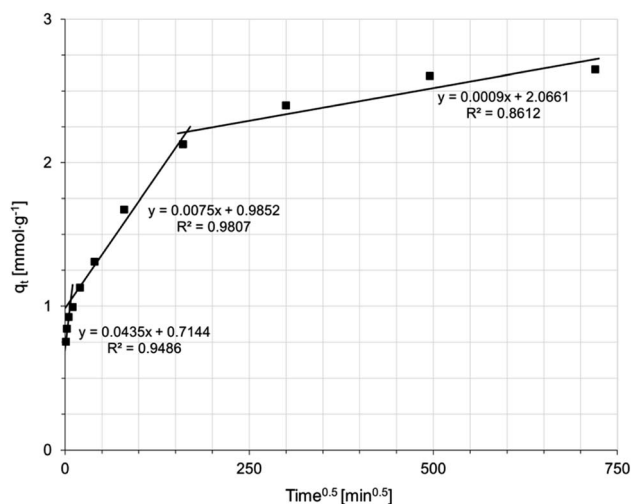
Table 5 Calculated diffusion rate constants for the adsorption of Ni(II) on AHP

Models	Parameters	Values
LFD	k_{LFD} (min^{-1})	4.20×10^{-3}
IPD	k_{IPD1} (mmol g^{-1} min^{-1})	4.35×10^{-2}
	k_{IPD2} (mmol g^{-1} min^{-1})	7.45×10^{-3}
	k_{IPD3} (mmol g^{-1} min^{-1})	0.91×10^{-3}

The constant rate values determined for each model (diffusion in the liquid film or intraparticle diffusion) suggest which step controls the entire Ni(II) ion removal process on the AHP. The values of the rate constants for each diffusion step are summarized in Table 5. The lowest value is taken by the parameter k_{IPD3}, indicating that the stage controlling the rate of the entire process corresponds to adsorption–desorption in equilibrium.

3.2.2. Static sorption

3.2.2.1 Effect of pH. The solution pH is a parameter strongly influencing the surface charge of the particles used for ion removal and additionally it controls the degree of ionization of the target ions in the working solution.[32] The effect of pH on the sorption of Ni(II) ions using AHP was determined in the pH range from 2.0 to 8.0 at a constant Ni(II) concentration (10 mM) and a constant amount of resin (40 mg). Fig. 7 shows the relationship between the initial pH of Ni(II) ion solutions and the adsorption capacity using the AHP resin. The sorption at pH above 8.0 was omitted due to possible disruption from Ni(OH)$_2$ precipitation in basic conditions. At pH lower than 8.0, Ni(II) ions are the dominant forms, and Ni(OH)$_2$ is present at pH higher than 8.0. The results showed that the maximum uptake of Ni(II) ions was observed when initial pH was set to 5.0, and the maximum sorption was 2.64 mmol g^{-1}. Under acidic conditions, the surface of the AHP is completely covered by H$^+$ ions, and Ni(II) ions due to lower concentration in relation to H$^+$ cannot compete for active sites. However, as pH increases, the concentration of H$^+$ does not disrupt the Ni(II) binding on active
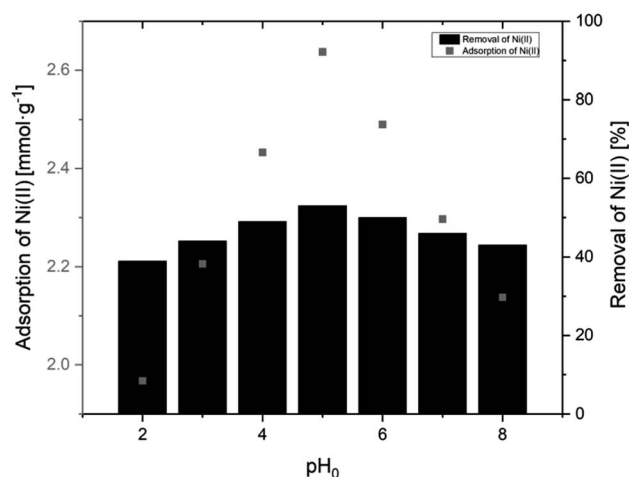

Fig. 6 Intraparticle diffusion model of Ni(II) sorption on AHP (initial Ni(II) concentration: 20 mM; concentration of resin: 4 mg dm^{-3}; 298 K; pH 5.0).

Fig. 7 Adsorption of Ni(II) onto AHP as a function pH (initial Ni(II) concentration:10 mM; concentration of resin: 4 mg dm^{-3}; 298 K).
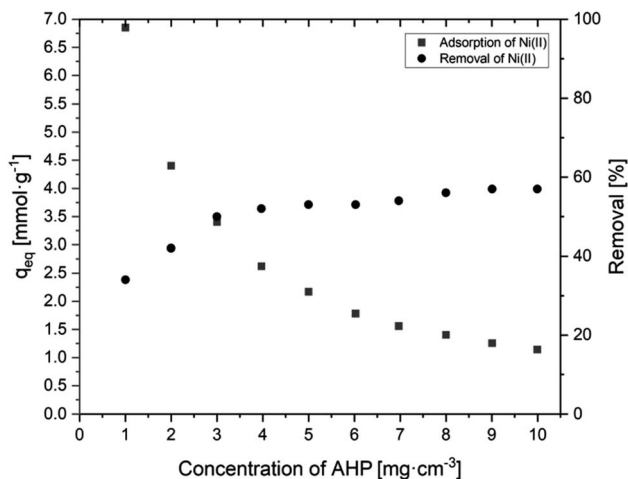
Fig. 8 Effect of AHP concentration of initial Ni(ɪɪ) concentration on sorption capacity of Ni(ɪɪɪ) and removal of Ni(ɪɪ) (initial Ni(ɪɪ) concentration: 20 mM; 298 K; pH 5.0).
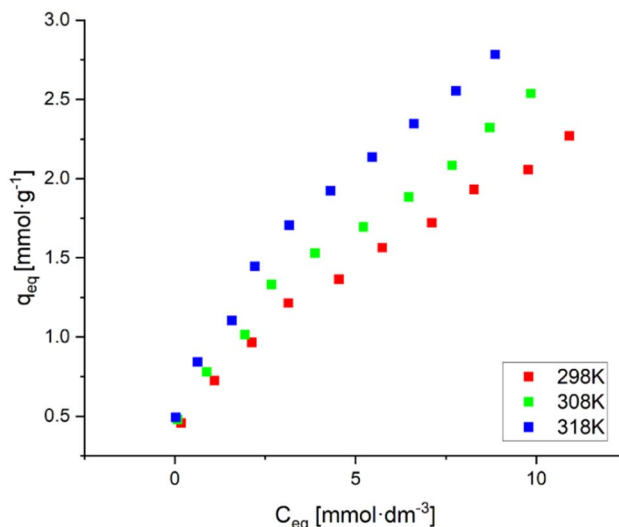

Fig. 9 Adsorption isotherms of Ni(ɪɪ) on AHP (initial Ni(ɪɪ) concentration: 20 mM; concentration of resin: 4 mg dm^{-3}; 298 K; pH 5.0).

sites and the removal is possible. Therefore, we observe an increase in the removal of Ni(ɪɪ) ions from an aqueous solution when the pH rises from 2.0 to 5.0 (Fig. 7).

3.2.2.2 Effect of resin dosage. Based on the obtained results shown in Fig. 8, it is evident that the percentage removal of Ni(ɪɪ) ions from the solution increases as the amount of resin increases. For the highest dose (10 g dm^{-3}), the highest ion removal of about 57.1% was obtained. It can also be observed that increasing the resin dose causes a decrease in the amount of adsorbed Ni(ɪɪ) ions. The highest amount of adsorbed Ni(ɪɪ) ions (6.85 mmol g^{-1}) is observed at the lowest resin dose (1 g dm^{-3}), while for an amount ten times higher, this value is only 1.14 mmol g^{-1}. A higher resin dose removes Ni(ɪɪ) ions more efficiently from the solution, but the amount of adsorbed ions per gram of the resin decreases, as there are not enough Ni(ɪɪ) ions to saturate all of the available active groups taking part in the removal process.

3.2.2.3 Effect of initial Ni(ɪɪ) ion concentration. After the effect of pH and resin dose amount on Ni(ɪɪ) ion removal was investigated, the effect of the initial Ni(ɪɪ) ion concentration in solution and temperature on the Ni(ɪɪ) ion removal process using AHP was determined. The obtained results are presented by sorption isotherms (Fig. 9). These data show that as the temperature increases, the sorption capacity increases. Thus, it can be concluded that increasing the temperature benefits the removal of Ni(ɪɪ) ions by AHP and indicates the endothermic nature of this sorption process. The visible increase in the sorption of Ni(ɪɪ) ions with increasing temperature is due to the acceleration of the diffusion of the removed molecules through the outer boundary layer caused by a decrease in the viscosity of the solution.[33] As a standard, it can be observed that as the initial Ni(ɪɪ) concentration in the solution increases, the amount of adsorbed ions increases. For the highest concentration, the highest values of 2.27, 2.54 and 2.78 mmol g^{-1} were achieved for 298, 308 and 318 K, respectively.

The obtained results were described by two isotherm models – Langmuir and Freundlich. The parameters of both models were determined using linear regression, and the Pearson correlation coefficient (R^2) was used as a criterion of fit. The Freundlich model performs well for adsorption at low concentrations. In contrast, the Langmuir model describes the behaviour of metal ions during ion exchange on resins. In addition, the Langmuir isotherm applies to ion exchange on an all-over homogeneous surface with inappreciable interaction between adsorbed molecules.[28] The calculated parameters, along with the R^2 value, are summarised in Table 6. The isotherms based on modelling results were added to the ESI as Fig. S2.†

The high values of the Pearson correlation coefficient for the isotherm models used ($R^2 > 0.95$) suggest that both models describe the experimental data well. The experimentally obtained sorption capacity of the AHP resin towards Ni(ɪɪ) ions (approximately 2.5 mmol g^{-1}) is higher than for commercial resins such as Dowex HCR-S,[34] Purolite NRW-100 (ref. 35) or Lewatit Monoplus SP112.[36] The sorption capacity of these resins ranges from 1.0 to 1.7 mmol g^{-1}.

3.2.2.4 Thermodynamics of Ni(ɪɪ) removal on AHP. The thermodynamic parameters including free energy (ΔG^0), enthalpy (ΔH^0), and entropy (ΔS^0) changes are indicators that can reveal the nature of Ni(ɪɪ) sorption on AHP. The free energy can be determined using eqn (4) whereas enthalpy change (ΔH^0) and entropy change (ΔS^0) can be extracted through graphical method from a plot of ln K_0 as a function of T^{-1} using slope and intercept values based on the eqn (5). Table 7 summarises the calculated thermodynamic parameters of Ni(ɪɪ) removal on AHP.

$$\Delta G^0 = -RT \ln K_0 \tag{4}$$

$$\ln K_0 = \frac{\Delta S^0}{R} - \frac{\Delta H^0}{RT} \tag{5}$$

Table 6 Parameters of isotherm adsorption models

	Langmuir isotherm			Freundlich isotherm		
T (K)	q_L (mmol g^{-1})	k_L (dm^3 mmol^{-1})	R^2 (−)	n (−)	k_F ((dm^3)$^{1/n}$ mmol$^{(1-1/n)}$ g^{-1})	R^2 (−)
298	2.39	0.371	0.960	2.05	0.679	0.995
308	2.52	0.468	0.952	2.07	0.792	0.981
318	2.62	0.689	0.970	2.17	0.989	0.990

Table 7 Thermodynamic parameters for process of Ni(II) ion removal onto AHP at different temperatures (298–318 K)

			Thermodynamic parameters		
T (K)	ln K_0 (−)	K_0 (−)	ΔG^0 (kJ mol^{-1})	ΔH^0 (kJ mol^{-1})	ΔS^0 (kJ mol^{-1} K^{-1})
298	0.987	2.68	−2.45	+28.3	−0.102
308	1.23	3.44	−3.16		
318	1.70	5.49	−4.50		

The Gibbs energy changes (ΔG^0) during the removal of Ni(II) on AHP at 298, 308, 318 K were negative, reveal a spontaneous nature of the process. The metal cations are driven to be bound to the resin more likely due to the higher affinity of Me^{2+} compared to hydrogen ions. The positive enthalpy change (ΔH^0) (+28.3 kJ mol^{-1}) indicates that the process is endothermic. The negative entropy change (ΔS^0) (−0.102 kJ mol^{-1} K^{-1}) suggests that an active complex is formed between Ni(II) ions and AHP during the process, indicating an association mechanism.[37] As reported in the literature, Ni(II) ion exchange occurring on various commercial resins (*e.g.* Lewatit Monoplus 112, Purolite NRW-100 or Dowex HCR-S) is mostly an endothermic process.[34–36,38]
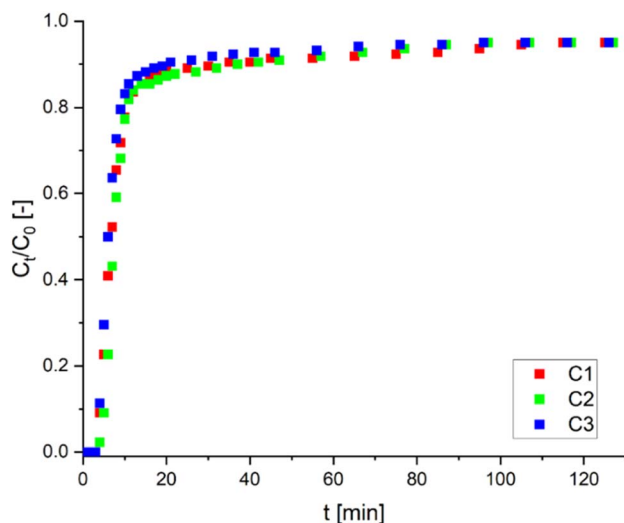
3.2.3. Dynamic sorption. The final step in studying the adsorption properties of AHP towards Ni(II) ions was to conduct measurements in a laboratory-scale fixed-bed column. The breakthrough curves for three cycles, *i.e.* the dependence of c_t/c_0 on the processing time (t), are shown in Fig. 10. Thus, the bed operation in the column was visualised. The curves show that a breakthrough was reached after 20 min of Ni(II) solution was passed through the column. The column capacity extracted from this experiment (0.92 mmol g^{-1}) is close to the capacity obtained from the batch experiments with comparable adsorbent-to-adsorbate ratio (0.012 g cm^{-3}) (Fig. 8).

After each adsorption cycle, the resin was regenerated to test its reusability. Regeneration with 25 mM HCl solution does not significantly affect the adsorption properties of the resin, and the sorption capacity is 0.920, 0.782 and 0.778 mmol g^{-1} for each cycle (C1, C2 and C3), respectively. After three successive adsorption–desorption cycles, the resin filled column retained about 85% of its original capacity. Furthermore, the high capacity retained after regeneration suggests that Ni(II) ions can be effectively removed without degrading the adsorbent structure. Breakthrough curves of three cycles (C1, C2 and C3) are presented in Fig. 10. The obtained results proved that the AHP resin could successfully remove Ni(II) ions from aqueous solutions in a reusable system.

3.2.4. Real wastewater treatment. The real wastewater treatment process is presented in Fig. 11. The real wastewater had twice as high concentration of Ni(II) ions compared to the
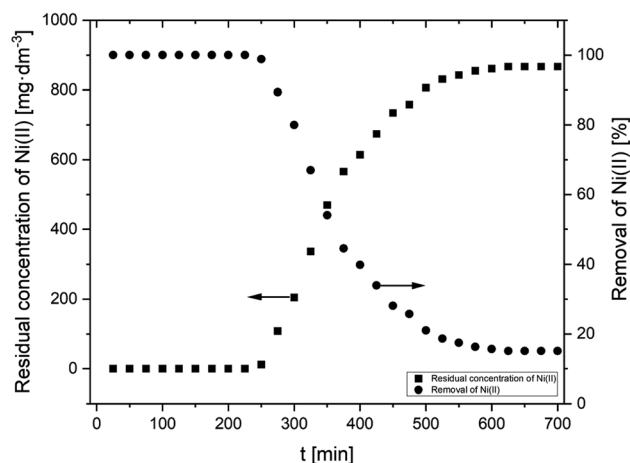
Fig. 10 Breakthrough curves for sorption of Ni(II) ions on AHP (flow rate of solution: 0.020 cm^3 s^{-1}; initial Ni(II) concentration: 11 mM; mass of resin: 1.5 g; 298 K; pH 5.0).

Fig. 11 Treatment of real wastewater containing Ni(II) ions using AHP (flow rate of solution: 0.020 cm^3 s^{-1}; initial Ni(II) concentration: 17.45 mM; mass of resin: 5 g; 298 K; pH 5.0).

model solutions, so a higher resin dose was used. The column bed of 5 g of AHP was enough to remove all the Ni(II) ions from 225 cm^3 of the solution at about 0.020 cm^3 s^{-1} flow. After 10 hours had passed, the breakthrough occurred as the Ni(II) was detected in the column effluent. As shown in Fig. 11, the real wastewater treatment process was carried out until the removal rate of Ni(II) ions stabilised at 15%. The maximum bed capacity was found to be 0.936 mmol g^{-1} in the dynamic mode with electroplating effluent.

4. Discussion

The obtained amino-hypophosphite polyampholyte (AHP) has good properties for removing Ni(II) ions from aqueous solutions in both batch and column systems for the treatment of both model solutions and real wastewater containing Ni(II) ions. This material has an easily permeable grainy form that allows medium aqueous flow through the fixed bed. It can be easily milled for desirable particle size depending on the chosen process parameters. Its density is higher than that of commercial ion scavengers, which could be an advantage in terms of the economy of transportation. The bulk density is comparable to commercial scavengers. The obtained material contains a substantial amount of active groups, that is, 5.7 mmol g^{-1} hypophosphite groups and 6.8 mmol g^{-1} amine groups. The structure of AHP has been confirmed by XPS analysis and ^{31}P NMR analysis and agrees with previously reported data.[27] AHP can be produced in proton or sodium form, which is an essential advantage in purification processes because of its ability to bind toxic cations and anions. It should also be noted that the reactions that result in AHP are simple and environmentally safe, which is a definite advantage given the importance of the principles of environmental protection and sustainability.
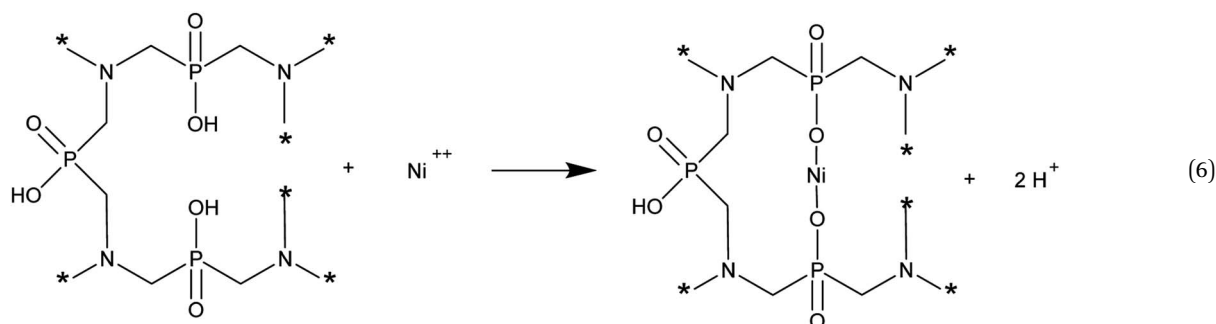
All sorption experiments carried out were aimed at indicating the applicability of the obtained AHP for the removal of Ni(II) ions from aqueous solutions. The kinetic experiment showed that the process of removing Ni(II) ions on AHP is very long and that equilibrium was reached after 24 hours. It can be observed that the removal efficiency does not increase significantly after 20 hours of exposure to a solution containing Ni(II) ions on AHP. The percentage of removal achieved after 24 hours under these process conditions (initial Ni(II) concentration: 20 mM; resin concentration: 4 mg dm^{-3}; 298 K; pH 5.0) was greater than 50%. Additionally, the calculated values of the rate constant for both the LFD and the IPD models indicate that the slowest stage is the third stage of the intraparticle diffusion assigned to the final stage of the adsorption–desorption equilibrium when diffusion slows down due to the low concentration of Ni(II) ions in solution. Given the moderate time required to reach equilibrium and that the obtained experimental kinetics data were consistent with the PSO model, it can be assumed that there is a chemical interaction between amino-hypophosphite polyampholyte and Ni(II) ions. Based on the results of the kinetic experiment, all batch experiments were conducted for 24 hours to allow a sorption equilibrium to be established in the system under study.

The removal of Ni(II) ions by physical, chemical or ion exchange mechanisms depends directly on the pH of the solution and the properties of the adsorbent. As reported by Cruz-Lopes and co-workers, nickel is a heavy metal whose sorption increases with increasing pH, and the most significant degree of removal is observed just before precipitation occurs.[39] The determination of the effect of pH on the removal of Ni(II) ions by AHP confirmed this finding and showed that the optimal pH for the process is 5.0. In an acidic solution, there is more competition between Ni(II) ions and H$^+$ ions for active sites on the AHP scaffolding. Thus, at lower pH (<3.0), the functional groups present in the resin structure bind to H$^+$ to a large extent, adversely affecting the process and resulting in lower sorption. At higher pH, when the H$^+$ concentration is reduced significantly, the less abundant Ni(II) are allowed to be bound to resin's active sites. Therefore, an increase in Ni(II) ion removal in an aqueous solution is observed when the pH increases from 2.0 to 5.0 (Fig. 7). It is worth noting that if the resin is in its proton form it releases H+ ions when the Ni(II) ions are bound to the materials, this causes pH to decrease during the process disrupting the process. This does not apply to sodium form of the resin. On the other hand, a decrease in sorption above pH 6.0 can be caused by precipitation of Ni(OH)$_2$, which ultimately hinders sorption, as the precipitate reduces accessibility to AHP active sites. Therefore, determining the optimal pH that promoted Ni(II) ion removal was crucial for the process to be carried out properly.

As studies have shown, in a batch sorption system, as the temperature increases, the maximum ionic capacity and removal efficiency are higher. Thus, increasing the temperature has a beneficial effect on the removal of Ni(II) ions on AHP. As expected, as the initial concentration of Ni(II) ions in the solution increases, the amount of adsorbed ions increases. The maximum ionic capacity of AHP at 318 K and 20 mM initial concentration of Ni(II) was 2.7 mmol g^{-1} and was calculated from the Langmuir isotherm. This capacity is high considering the theoretical ionic capacity calculated from the abundance of hydroxyl fragments of hypophosphite groups (2.9 mmol g^{-1}). This indicates that the removal process is partly based on simple ion exchange (the change in solution pH during removal of Ni(II) ions by AHP). However, it can be assumed that the complexation mechanism also contributes significantly to Ni(II) removal on AHP. Chemical interactions between Ni(II) ions and AHP are also confirmed by thermodynamic analysis of the process. The total free energy changes (ΔG^0) during the sorption of Ni(II) ions on AHP at all temperatures studied were negative, indicating a spontaneous process of Ni(II) ion removal from solution, and the removed cations are more favourably bound to AHP compared to protons.[33] A positive enthalpy change (ΔH^0) indicates that the process is endothermic. In contrast, a negative entropy change (ΔS^0) value suggests that an active complex is formed between Ni(II) ions and AHP during the process. This indicates an associative mechanism in which the Ni(II) ions are initially attached to the active site and release of the receding ions occurs. As a heavy metal, nickel is prone to associative

reactions. Given this information, a mechanism for the removal of Ni(II) ions on AHP can be proposed according to the following scheme:

experiment shows that AHP has great potential to recover Ni(II) and reduce the volume of wastewater containing toxic metal ions.

$$+ \quad Ni^{++} \quad \longrightarrow \quad + \quad 2\,H^+ \qquad (6)$$

In the final step of investigating the adsorption properties of AHP towards Ni(II) ions, experiments were carried out in a laboratory-scale fixed-bed column. The dry resin introduced into the column (1.5 g) occupied 0.026 m, while when contacted with the solution, it swelled to reach a height of 0.065 m; *i.e.* the height of the bed in the column was 2.5 times higher than initially. The Ni(II) concentration distribution curves shown in Fig. 10 are typical relationships for the sorption process, where three characteristic zones can be distinguished. The first zone, the moment of the column breakthrough, is when the functional groups on the AHP are saturated with Ni(II) ions from the solution (up to 2 minutes). Then a surge is seen, forming an ion exchange zone and running for up to 20 minutes. A third zone is visible after 20 minutes, when the concentration decay curve flattens out, thereby decreasing the efficiency of the process, and the concentration of Ni(II) ions in the solution leaving the column is about 95% of the initial concentration. The same trend is seen in each cycle. The breakthrough curves are very close to each other, indicating the effective regeneration of the resin with an HCl solution. After three successive adsorption–desorption cycles, the column retained about 85% of its original capacity. Furthermore, the high capacity retained after regeneration suggests that Ni(II) ions can be effectively removed without degrading the adsorbent's structure.

The process parameters obtained from batch and dynamic mode experiments allowed us to conduct a successful recovery of Ni(II) from electroplating effluent. The maximum bed capacity obtained during treatment in the dynamic system of real galvanic wastewater was found to be 0.936 mmol g^{-1}. This value is similar to the capacity obtained during the model wastewater treatment on the AHP. It is also worth noting that the fraction collected from the column regeneration was 7 times more concentrated than the feed. If the experiment had been stopped at the breakthrough point, the concentration factor obtained could have been even higher. This laboratory-scale

5. Conclusions

The obtained amino-hypophosphite polyampholyte (AHP), a derivative of bis(hexamethylene)triamine, is a material with excellent properties that enable it to be implemented to metal ions removal processes from aqueous solutions. The tests carried out in the batch and column systems showed a good affinity of AHP for Ni(II) ions. The adsorbed amount of Ni(II) ions reached peak values at pH values between 4 and 6 for the studied AHP. Therefore, pH ∼5.0 is recommended for sorption studies. With increasing temperature, the sorption of Ni(II) ions increased for AHP, revealing the endothermic nature of the removal process. In the investigated Ni(II) ion concentration range and resin dosage, the Pearson correlation coefficients (R^2) for the Langmuir and Freundlich models were acceptable ($R^2 >$ 0.95). The maximum sorption capacity was calculated from the Langmuir isotherm and was 2.39, 2.52, and 2.62 mmol g^{-1} for 298, 308 and 318 K, respectively. The time to reach equilibrium in the studied system was moderate at 24 hours. The pseudo-second order kinetic model well described the kinetic data, and the process was found to be controlled by the adsorption–desorption equilibrium. Experiments in a fixed bed column show that AHP can successfully recover Ni(II) ions from model solutions and galvanic wastewater. Furthermore, after washing the AHP loaded with Ni(II) ions with a small amount of 6 M HCl, a highly concentrated nickel solution with a concentration of 7.3 g dm^{-3} can be obtained, significantly reducing the volume of wastewater. The concentrate can be further treated to remove unwanted ions and reintroduce them into the process. The research showed that amino-hypophosphite polyampholyte (AHP) could be an alternative material for scavenging Ni(II) ions from aqueous solutions. It is obtained safely and quickly from cheap materials and exhibits properties similar to those of commercial ion exchange or chelating resins derived from petroleum.

Abbreviations

B	Parameter related to the thickness of the boundary layer (mmol g^{-1})
c	Concentration of Ni(II) (mmol dm^{-3})
c_0	Initial concentration of Ni(II) (mmol dm^{-3})
c_e	Equilibrium concentration of Ni(II) (mmol dm^{-3})
F	Fractional attainment of equilibrium ($-$)
K_0	Equilibrium constant ($-$)
k_1	Rate constant of the PFO model (min^{-1})
k_2	Rate constant of the PSO model (g $mmol^{-1}$ min^{-1})
k_F	Freundlich constant indicative of the relative adsorption capacity of the adsorbent (($dm^3)^{1/n}$ $mmol^{(1-1/n)}$ g^{-1})
k_{IPD}	Intraparticle diffusion rate constant (mmol g^{-1} min^{-1})
k_L	Langmuir constant related to the energy of adsorption (dm^3 $mmol^{-1}$)
k_{LFD}	Liquid film diffusion rate constant (min^{-1})
m	Mass of AHP (g)
n	Freundlich equation exponent ($-$)
PR	Percentage removal of Ni(II) (%)
q	Amount of Ni(II) adsorbed (mmol g^{-1})
q_1	Adsorption capacity of Ni(II) for PFO model (mmol g^{-1})
q_2	Adsorption capacity of Ni(II) for PSO model (mmol g^{-1})
q_e	Amount of Ni(II) adsorbed at equilibrium (mmol g^{-1})
q_{exp}	Amount of adsorbed Ni(II) obtained experimentally (mmol g^{-1})
q_L	Maximum adsorption capacity in the Langmuir model (mmol g^{-1})
q_t	Amount of Ni(II) adsorbed at time t (mmol g^{-1})
R	Universal gas constant (kJ mol^{-1} K^{-1})
t	Time (min)
T	Temperature (K)
V	Solution volume (dm^3)
ΔG^0	Free energy (kJ mol^{-1})
ΔH^0	Enthalpy (kJ mol^{-1})
ΔS^0	Entropy (kJ mol^{-1} K^{-1})

Author contributions

JU: conceptualization, investigation, methodology, visualization, writing – original draft, resources. ŁS: methodology, investigation, visualization, writing – original draft, writing – review & editing. NT: investigation, visualization, writing – original draft. IP: writing – review & editing.

Conflicts of interest

There are no conflicts to declare.

Acknowledgements

References

1 H. B. Bradl, Chapter 1 Sources and origins of heavy metals, *Interface Sci. Technol.*, 2005, **6**, 1–27, DOI: 10.1016/s1573-4285(05)80020-1.

2 G. M. Gadd, Heavy Metal Pollutants: Environmental and Biotechnological Aspects, *Reference Module in Life Sciences*, 2017, vol. 3, pp. 321–334, DOI: 10.1016/b978-0-12-809633-8.13057-2.

3 A. S. Mohammed, A. Kapri and R. Goel, Heavy Metal Pollution: Source, Impact, and Remedies, *Biomanagement of Metal-Contaminated Soils*, 2011, pp. 1–28, DOI: 10.1007/978-94-007-1914-9_1.

4 J. H. Duffus, Heavy metals—a meaningless term?, *Chem. Int.*, 2001, **23**(6), 163–167, DOI: 10.1515/ci.2001.23.6.163.

5 P. B. Tchounwou, C. G. Yedjou, A. K. Patlolla and D. J. Sutton, Heavy Metal Toxicity and the Environment, *Molecular, Clinical and Environmental Toxicology*, 2012, vol. 101, pp. 133–164, DOI: 10.1007/978-3-7643-8340-4_6.

6 C. Klein and M. Costa, Nickel**Revised and updated from the chapter by Tor Norseth, 1986 edition of this Handbook. *Handbook on the Toxicology of Metals*, 2007, pp. 743–758, DOI: 10.1016/b978-012369413-3/50090-2.

7 G. Genchi, A. Carocci, G. Lauria, M. S. Sinicropi and A. Catalano, Nickel: Human Health and Environmental Toxicology, *Int. J. Environ. Res. Public Health*, 2020, **17**(3), 679, DOI: 10.3390/ijerph17030679.

8 D. G. Barceloux and D. Barceloux, Nickel, *J. Toxicol., Clin. Toxicol.*, 1999, **37**(2), 239–258, DOI: 10.1081/clt-100102423.

9 K. H. Vardhan, P. S. Kumar and R. C. Panda, A review on heavy metal pollution, toxicity and remedial measures: Current trends and future perspectives, *J. Mol. Liq.*, 2019, **290**, 111197, DOI: 10.1016/j.molliq.2019.111197.

10 R. Khlifi and A. Hamza-Chaffai, Head and neck cancer due to heavy metal exposure via tobacco smoking and professional exposure: A review, *Toxicol. Appl. Pharmacol.*, 2010, **248**(2), 71–88, DOI: 10.1016/j.taap.2010.08.003.

11 W. Yuan, N. Yang and X. Li, Advances in Understanding How Heavy Metal Pollution Triggers Gastric Cancer, *BioMed Res. Int.*, 2016, 1–10, DOI: 10.1155/2016/7825432.

12 H. J. Lee, M. K. Park and Y. R. Seo, Pathogenic Mechanisms of Heavy Metal Induced-Alzheimer's Disease, *J. Toxicol. Environ. Health Sci.*, 2018, **10**(1), 1–10, DOI: 10.1007/s13530-018-0340-x.

13 M. T. Kabir, M. S. Uddin, S. Zaman, Y. Begum, G. M. Ashraf, M. N. Bin-Jumah, *et al.*). Molecular Mechanisms of Metal Toxicity in the Pathogenesis of Alzheimer's Disease, *Mol. Neurobiol.*, 2021, **58**, 1–20, DOI: 10.1007/s12035-020-02096-w.

14 M. Saito, R. Arakaki, A. Yamada, T. Tsunematsu, Y. Kudo and N. Ishimaru, Molecular Mechanisms of Nickel Allergy, *Int. J. Mol. Sci.*, 2016, **17**(2), 202–210, DOI: 10.3390/ijms17020202.

15 N. Rahmati, M. Rahimnejad, M. Pourali and S. K. Muallah, Effective removal of nickel ions from aqueous solution using multi-wall carbon nanotube functionalized by

glycerol-based deep eutectic solvent, *Colloid Interface Sci. Commun.*, 2021, **40**, 100347, DOI: **10.1016/j.colcom.2020.100347**.

16 K. C. Khulbe and T. Matsuura, Removal of heavy metals and pollutants by membrane adsorption techniques, *Appl. Water Sci.*, 2018, **8**(1), 19–49, DOI: **10.1007/s13201-018-0661-6**.

17 E.-S. Salama, H.-S. Roh, S. Dev, M. A. Khan, R. A. I. Abou-Shanab, S. W. Chang and B.-H. Jeon, Algae as a green technology for heavy metals removal from various wastewater, *World J. Microbiol. Biotechnol.*, 2019, **35**(5), 75–88, DOI: **10.1007/s11274-019-2648-3**.

18 N. Abdullah, N. Yusof, W. J. Lau, J. Jaafar and A. F. Ismail, Recent trends of heavy metal removal from water/wastewater by membrane technologies, *J. Ind. Eng. Chem.*, 2019, **76**, 17–38, DOI: **10.1016/j.jiec.2019.03.029**.

19 S. Y. Cheng, P.-L. Show, B. F. Lau, J.-S. Chang and T. C. Ling, New prospects for modified algae in heavy metal adsorption, *Trends Biotechnol.*, 2019, **37**, 1255–1268, DOI: **10.1016/j.tibtech.2019.04.007**.

20 R. Alfarra, N. Ali and M. Yusoff, Removal of heavy metals by natural adsorbent: review, *Int. J. Biosci.*, 2014, **4**(7), 130–139, DOI: **10.12692/ijb/4.7.130-139**.

21 S. Kumar and S. Jain, History, Introduction, and Kinetics of Ion Exchange Materials, *J. Chem.*, 2013, 1–13, DOI: **10.1155/2013/957647**.

22 V. Veselý, Synthetic inorganic ion-exchangers—I Hydrous oxides and acidic salts of multivalent metals, *Talanta*, 1972, **19**(3), 219–262, DOI: **10.1016/0039-9140(72)80075-4**.

23 V. Neagu, I. Bunia and C. Luca, Organic Ion Exchangers. Synthesis and Their Behaviour in the Retention of Some Metal Ions, *Macromol. Symp.*, 2006, **235**(1), 136–142, DOI: **10.1002/masy.200650317**.

24 *Global Ion Exchange and Adsorption Separation Resin Market Report, History and Forecast 2018-2029, Breakdown Data by Manufacturers, Key Regions, Types and Application*, PUBLISHER: QYResearch, 2023, **https://www.qyresearch.com/reports/1474341/ion-exchange-and-adsorption-separation-resin** (accessed August 10, 2023).

25 *Global Metal Scavenger Market Research Report 2023*, PUBLISHER: QYResearch, 2023. **https://www.qyresearch.com/reports/421392/metal-scavenger** (accessed August 10, 2023).

26 Ł. Stala, J. Ulatowska and I. Polowczyk, A review of polyampholytic ion scavengers for toxic metal ion removal from aqueous systems, *Water Res.*, 2021, **203**, 117523, DOI: **10.1016/j.watres.2021.117523**.

27 Ł. Stala, J. Ulatowska and I. Polowczyk, Copper(II) ions removal from model galvanic wastewater by green one-pot synthesised amino-hypophosphite polyampholyte, *J. Hazard. Mater.*, 2022, **436**, 1–15, DOI: **10.1016/j.jhazmat.2022.129047**.

28 E. Pehlivan and T. Altun, Ion-exchange of Pb^{2+}, Cu^{2+}, Zn^{2+}, Cd^{2+}, and Ni^{2+} ions from aqueous solution by Lewatit CNP 80, *J. Hazard. Mater.*, 2007, **140**, 299–307, DOI: **10.1016/j.jhazmat.2006.09.011**.

29 A. Pholosi, E. B. Naidoo and A. E. Ofomaja, Intraparticle diffusion of Cr(VI) through biomass and magnetite coated biomass: A comparative kinetic and diffusion study, *S. Afr. J. Chem. Eng.*, 2020, **32**, 39–55, DOI: **10.1016/j.sajce.2020.01.005**.

30 T. Tarawou and E. Young, Intraparticle and liquid film diffusion studies on the adsorption of Cu^{2+} and Pb^{2+} ions from aqueous solution using powdered cocoa pod (*Theobroma cacao*), *Int. Res. J. Eng. Tech.*, 2015, **2**(8), 236–243.

31 H. ., L. V. Qiu, B. Pan, Q. Zhang, W. Zhang and Q. Zhang, Critical review in adsorption kinetic models, *J. Zhejiang Univ., Sci., A*, 2009, **10**, 716–724, DOI: **10.1631/jzus.A0820524**.

32 S. Banerjee and M. C. Chattopadhyaya, Adsorption characteristics for the removal of a toxic dye, tartrazine from aqueous solutions by a low cost agricultural by-product, *Arabian J. Chem.*, 2017, **10**, S1629–S1638, DOI: **10.1016/j.arabjc.2013.06.005**.

33 V. G. Georgieva, L. Gonsalvesh and M. P. Tavlieva, Thermodynamics and kinetics of the removal of nickel (II) ions from aqueous solutions by biochar adsorbent made from agro-waste walnut shells, *J. Mol. Liq.*, 2020, **312**, 112788, DOI: **10.1016/j.molliq.2020.112788**.

34 G. A. Fil, R. Boncukcuoğlu, A. E. Yilmaz and S. Bayar, Adsorption of Ni(II) on ion exchange resin: Kinetics, equilibrium and thermodynamic studies, *Korean J. Chem. Eng.*, 2012, **29**(9), 1232–1238, DOI: **10.1007/s11814-012-0012-5**.

35 R.-S. Juang, H.-C. Kao and F.-Y. Liu, Ion exchange recovery of Ni(II) from simulated electroplating waste solutions containing anionic ligands, *J. Hazard. Mater.*, 2006, **128**(1), 53–59, DOI: **10.1016/j.jhazmat.2005.07.027**.

36 D. Kołodyńska, D. Fila and Z. Hubicki, Recovery of lanthanum(III) and nickel(II) ions from acidic solutions by the highly effective ion exchanger, *Molecules*, 2020, **25**(16), 3718, DOI: **10.3390/molecules25163718**.

37 P. Saha, S. Chowdhury and T. Mizutani, Insight into adsorption thermodynamics, in *Thermodynamics*, ed. M. Tadashi, InTech, Rijeka, 2011, pp. 349–364, DOI: **10.5772/13474**.

38 N. Dizge, B. Keskinler and H. Barlas, Sorption of Ni(II) ions from aqueous solution by Lewatit cation-exchange resin, *J. Hazard. Mater.*, 2009, **167**, 915–926, DOI: **10.1016/j.jhazmat.2009.01.073**.

39 L. P. Cruz-Lopes, M. Macena, B. Esteves and R. P. F. Guiné, Ideal pH for the adsorption of metal ions Cr6+, Ni2+, Pb2+ in aqueous solution whit different adsorbent materials, *Open Agric. J.*, 2021, **6**(1), 115–123, DOI: **10.1515/opag-2021-0225**.